

## Spin reorientation and crystal field in the single-crystal hydride $\text{HoFe}_{11}\text{TiH}$

S. A. Nikitin,<sup>1,2,\*</sup> I. S. Tereshina,<sup>1,2</sup> N. Yu. Pankratov,<sup>1</sup> and Yu. V. Skourski<sup>1,2</sup>  
<sup>1</sup>*Department of Physics, Moscow State University, Vorobyevy Gory, 119899, Moscow, Russia*  
<sup>2</sup>*International Laboratory of High Magnetic Fields and Low Temperatures, Wroclaw, Poland*

(Received 30 November 2000; published 7 March 2001)

We present a study of the hydrogenation effect on structural and magnetic properties of  $\text{HoFe}_{11}\text{Ti}$  single crystal. Single crystal hydride  $\text{HoFe}_{11}\text{TiH}_x$  with H concentration  $x=1$  at. H/f.u. has been prepared. Magnetization measurements along the main symmetry directions of the tetragonal structure have been performed on  $\text{HoFe}_{11}\text{TiH}_x$  ( $x=0,1$ ) single crystals at applied high magnetic fields up to 80 kOe in the temperature range from 4.2 to 300 K. Torque measurements were carried out in the temperature range 78–700 K in magnetic fields up to 13 kOe. The single-ion magnetic exchange and crystalline-electric-field interaction model has been applied to the fitting of the experimental behavior of the single-crystal  $\text{HoFe}_{11}\text{TiH}_x$  ( $x=0,1$ ) samples. A set of CEF parameters and mean exchange field has been obtained. Hydrogen atoms have been found to have a significant effect on the second-order crystal field parameter  $A_2^0$  ( $A_2^0 = -20.5 \text{ Ka}_0^{-2}$  for  $\text{HoFe}_{11}\text{Ti}$  and  $A_2^0 = -118 \text{ Ka}_0^{-2}$  for  $\text{HoFe}_{11}\text{TiH}$ ).

DOI: 10.1103/PhysRevB.63.134420

PACS number(s): 75.30.Gw

One of the most important recent developments in the field of magnetism and magnetic materials has been the realization that improvement in magnetic properties can be achieved by introducing into the intermetallic compounds crystalline lattice of light interstitial elements (hydrogen, nitrogen, carbon). This is particularly necessary for powerful magnet materials such as the  $R_2\text{Fe}_{14}\text{B}$ ,  $R_2\text{Fe}_{17}$ , and also materials characterized by the formula  $R\text{Fe}_{12-x}\text{T}_x$  ( $T=\text{Al, Ti, V, Cr, Mo, W, and Si}$ ) with tetragonal crystal structure of the  $\text{ThMn}_{12}$  type. The compounds of the last group exhibit all peculiarities of the magnetic properties of rare-earth intermetallics with high  $3d$  metal content from the structural viewpoint being much more simple than earlier mentioned related compounds ( $R_2\text{Fe}_{14}\text{B}$  and  $R_2\text{Fe}_{17}$ ). The crystallographic structure of the  $\text{ThMn}_{12}$  type presents only one high-symmetry ( $14/mmm$ ) site for the rare-earth ions, thus eliminating all possible competition between different rare-earth sites.

The origin of magnetocrystalline anisotropy energy in these compounds is believed to be directly related to an interaction between the  $4f$  electrons and the crystal field. This interaction can be fully described by the crystal electric field (CEF) parameters. Examples of crystal-field analysis of the experimental behavior of single-crystal samples can be found for  $R_2\text{Fe}_{14}\text{B}$ ,<sup>1–3</sup>  $R_2\text{Fe}_{17}$ ,<sup>4</sup> and also for the  $R\text{Fe}_{12-x}\text{T}_x$  (in the case where  $T=\text{Ti}$  and  $x=1$ ).<sup>5,6</sup> Until now no single crystals of the hydrogen containing compounds were available. Hydrides of the anisotropic materials with high  $3d$  metal content have been systematically investigated only on a polycrystalline samples.<sup>7–9</sup>

We have prepared the  $R\text{Fe}_{11}\text{TiH}_x$  hydrides without deprecipitation of the single-crystal samples.<sup>10</sup> In this work we have investigated two fundamental aspects of the hydrogenated materials. These are the effect of hydrogen interstitials on the (i) crystalline electric field and (ii) exchange interactions. We will focus our study on  $\text{HoFe}_{11}\text{Ti}$  intermetallic since well characterized and good quality single crystals were obtained.

Details of single crystal preparation have been described

previously in Ref. 11. Purified hydrogen obtained by decomposition of  $\text{LaNi}_5\text{H}_x$  was used for hydrogenation. The sample was activated at  $T=473$  K in a vacuum and then hydrogenated at the same temperature under a hydrogen pressure of  $3 \times 10^5$  Pa. The obtained single crystal hydride was  $\text{HoFe}_{11}\text{TiH}_x$  at  $x \approx 1$ . The concentration of absorbed hydrogen in the samples was calculated using the Van der Waals equation and additionally was measured by full burning method.

X-ray diffraction experiments with  $\text{CuK}_\alpha$  radiation were made for the phase identification both of the parent compounds and their hydrides and to determine unit cell parameters. The samples were used in the shape of a disk and sphere approximately 3–4 mm in diameter. Thermomagnetic analysis (TMA) was used to measure the Curie temperature in a field of 1 kOe. The magnetic measurements were carried out in temperature range 4.2–300 K and in magnetic field up to 80 kOe on standard equipment. Torque measurements were carried out in the temperature range 77–700 K in magnetic fields up to 13 kOe on single crystals. All the data were corrected for the demagnetizing field.

$\text{HoFe}_{11}\text{Ti}$  compounds was found to be crystallized in the tetragonal  $\text{ThMn}_{12}$ -type structure. Lattice constants  $a$  and  $c$ , unit cell volume  $V$  are listed in Table I. It was observed that the hydrogenation leads to a lattice expansion of the compounds without change of the tetragonal structure of the  $\text{ThMn}_{12}$  type. The  $c/a$  ratio of the host alloys at room temperature was determined to be slightly reduced upon hydrogenation. This indicated that hydrogen expanded the lattice more along the  $a$  axis than the  $c$  axis. A neutron diffraction investigation<sup>12</sup> showed that hydrogen occupies the octahe-

TABLE I. Crystallographic data of the  $\text{HoFe}_{11}\text{Ti}$  compound and its hydride.

Compound	$a$ (nm)	$c$ (nm)	$c/a$	$V$ (nm <sup>3</sup> )	$\Delta V/V$ (%)
$\text{HoFe}_{11}\text{Ti}$	0.846	0.475	0.5615	0.3399	
$\text{HoFe}_{11}\text{TiH}$	0.850	0.476	0.5600	0.3439	1.1

TABLE II. Magnetic data of the  $\text{HoFe}_{11}\text{Ti}$  compound and its hydride.

Compound	$\sigma_S$ , emu/g		$T_C$ , K	$T_{SR}$ , K	Easy direction of magnetization	
	$T=4.2$ K	$T=300$ K			$T=4.2$ K	$T=300$ K
$\text{HoFe}_{11}\text{Ti}$	75.6	84.5	518		axial	axial
$\text{HoFe}_{11}\text{TiH}$	83.3	93	561	140	cone	axial

dron  $2b$  sites in the  $\text{HoFe}_{11}\text{Ti}$  lattice. The relative cell volume increases  $\Delta V/V$ , also shown in Table I, shows a consistent  $\sim 1.1\%$  volume expansion over the hydrogen-free unit cell.

The compounds  $\text{HoFe}_{11}\text{Ti}$  and  $\text{HoFe}_{11}\text{TiH}$  are ferrimagnets with a Curie temperature  $T_C$  of 518 and 561 K, respectively. Curie temperatures  $T_C$  and saturation magnetizations  $\sigma_S$  of the  $\text{HoFe}_{11}\text{Ti}$  compounds and its hydride are listed in Table II.

It is known that  $T_C$  is very sensitive to the Fe-Fe distance, and the  $T_C$  increase after hydrogenation is attributed to the increase of the exchange interaction between  $3d$  ions. The saturation magnetization was enhanced upon hydrogenation (see Table II). Arnold *et al.*<sup>13</sup> reported that, on the contrary, a decrease of the magnetization of  $\text{HoFe}_{11}\text{Ti}$  compounds with pressure was observed. In addition to the size effect, the change of saturation magnetization may be conditioned by the transformation of electronic structure of the  $\text{HoFe}_{11}\text{Ti}$  intermetallic compound.

Magnetocrystalline anisotropy is one of the most important intrinsic magnetic properties. In the  $\text{HoFe}_{11}\text{Ti}$  compounds Boltich *et al.*<sup>14</sup> found a second-order SRT from an ‘‘easy axis’’ to an ‘‘easy cone’’ at  $T_{\text{SRT}}=52$  K, but several authors<sup>5,6,15</sup> reported that the easy magnetization direction (EMD) remains along the  $c$  axis in the whole magnetic ordering temperature range. Our measurements on single crystals confirm the latter view. Such a behavior is consistent

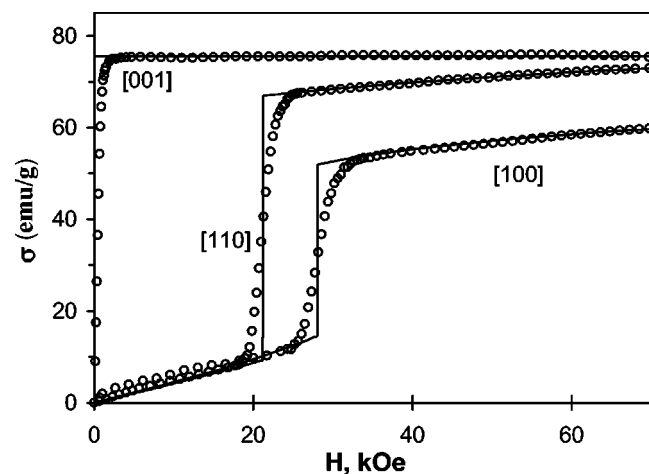


FIG. 1. Magnetization isotherms for the  $\text{HoFe}_{11}\text{Ti}$  single crystal for the magnetic field applied along the three main symmetry directions at  $T=4.2$  K (the lines is calculated).

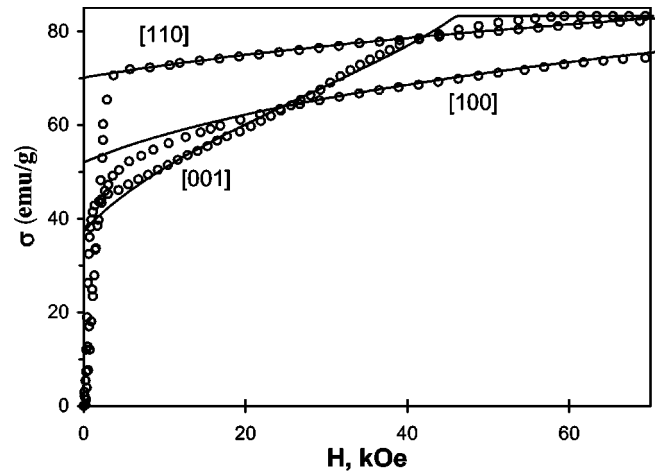


FIG. 2. Magnetization isotherms for the  $\text{HoFe}_{11}\text{TiH}$  single crystal for the magnetic field applied along the three main symmetry directions at  $T=4.2$  K (the lines is calculated).

with large variation of the SRT temperature  $T_{\text{SRT}}$  observed by varying the Ti content in titanium-stabilized  $R\text{Fe}_{12-x}\text{Ti}_x$  compounds (see Ref. 16). We investigated single crystals obtained by means of x-ray microanalysis using Cameca installation. The x-ray microanalysis of the samples reveals that they correspond to the formula  $\text{Ho}_{1.03}\text{Fe}_{11}\text{Ti}_{0.96}$ . Thus small deviations from nominal composition were found.

The experimental isotherms for the  $\text{HoFe}_{11}\text{Ti}$  and its hydride have been obtained at some selected temperatures (4.2, 40, 80, 120, 160, 200, and 300 K). Figures 1 and 2 show, for example, the isotherms obtained from the magnetization measurements for  $\text{HoFe}_{11}\text{Ti}$  single crystal and its hydride, correspondingly, for the magnetic field applied along the three main symmetry directions [100], [110], and [001] at  $T=4.2$  K. The easy magnetization direction corresponds to the [001] axis for  $\text{HoFe}_{11}\text{Ti}$ . A field-induced first-order magnetization process (FOMP) in a hard-magnetization direction

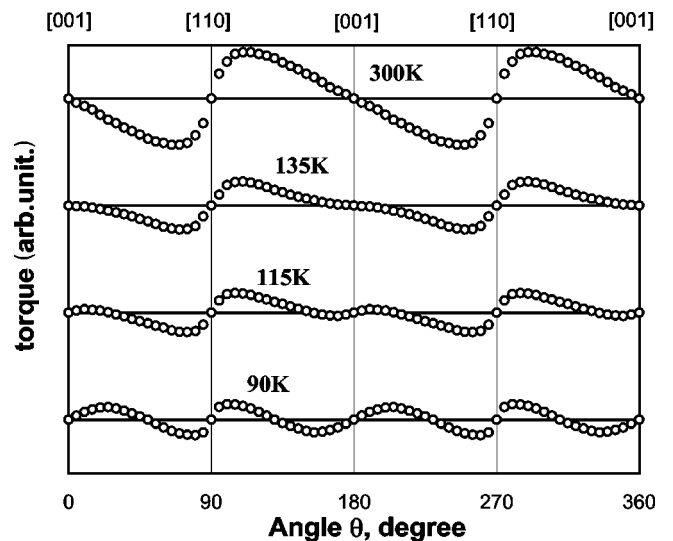


FIG. 3. Torque curves for single crystal hydride  $\text{HoFe}_{11}\text{TiH}$  at several selected temperatures:  $T=90, 115, 135, 300$  K at  $H=12$  kOe.

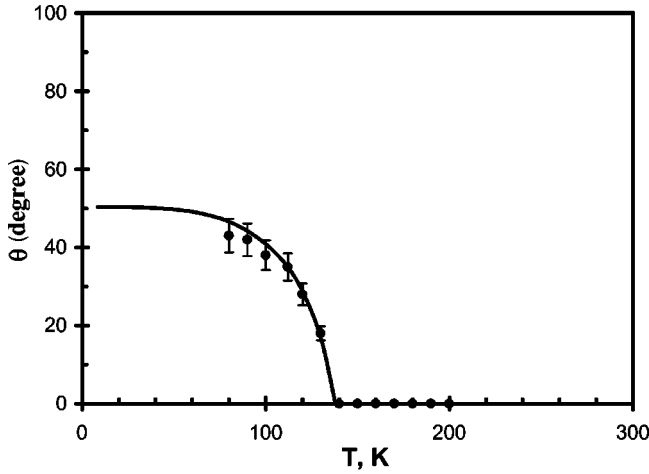


FIG. 4. Comparison of the experimental and calculated angle  $\theta$  of spin reorientation [the line is calculated using formula (A5) reproduced in Ref. 17].

is observed. There exists a strong MCA in the basal plane. Drastic changes in the magnetization are observed after the interstitial element insertion, which indicated the complicated magnetic structure of single crystal  $\text{HoFe}_{11}\text{TiH}$  hydride.

Torque magnetometry was used to study the MCA behavior. The temperature variation of the observed torque curves  $L(\theta)$ , for  $\text{HoFe}_{11}\text{TiH}$  (010)—disk specimens are shown in Fig. 3, where  $\theta$  is the angle between  $c$  axes and the magnetization vector. From this figure it is seen that the shape of the torque curves at high temperatures are quite different from those at low temperatures. At  $T=300$  K the shape of torque curve was a typical uniaxial type ([001] and [110] are the easy and hard directions, respectively), while that at low temperatures ( $T=90$ – $135$  K) was more complicated. The easy axis determined as the intercept of the  $\theta$  axis and the curve  $L(\theta)$  where. Here  $L(\theta)$  changes from positive to negative with increasing  $\theta$ . Thus, the temperature variation of the easy magnetization axis is immediately seen from Fig. 4. The solid line in Fig. 4 is calculated using formula (A5) reproduced in Ref. 17. The spin reorientation occurs as a second-order transition at  $T_{\text{SRT}}=140$  K.

Theoretical calculations were made to explain this anisotropy behavior. The method used to analyze the data is the mean-field approximation including exchange and crystal-field interaction, which was successfully applied and fully described for  $\text{HoFe}_{11}\text{Ti}$  in Ref. 6. The exchange field  $H_{\text{ex}}(0)$  and crystal field parameters  $A_n^m$ , where  $A_n^m = B_n^m / \theta_n \langle r^n \rangle$  ( $\theta_n$  are the Stevens coefficients and  $\langle r^n \rangle$  are the Hantree-Fork radial integrals) used to fit the experimental data for magnetization isotherms are shown in Table III.

TABLE III. Crystal electric field coefficient  $A_n^m$  (in  $\text{Ka}_0^{-n}$  units) and exchange field between  $3d$  and  $4f$  sublattices  $\mu_B H_{\text{ex}}$  (in  $K$  units). The data of the  $\text{HoFe}_{11}\text{Ti}$  compound have been reported in Ref. 6.

Compounds	$A_2^0$	$A_4^0$	$A_6^0$	$A_4^4$	$A_6^4$	$\mu_B H_{\text{ex}}(0)$
$\text{HoFe}_{11}\text{Ti}$	-20.5	-11.1	5.02	-153.2	-0.81	100
$\text{HoFe}_{11}\text{TiH}$	-118.0	-8.6	1.4	-200.0	-0.85	112

A comparison of the experimental results shown in Figs. 1 and 2 (open circles) with calculated data (solid lines) clearly shows that the model using five crystal field parameters does an excellent job of reproducing the experimental results. The main feature that emerges, confirming previous investigations, is the small value of the second-order crystal-field parameters for  $R\text{Fe}_{11}\text{Ti}$  and hence the importance of higher-order terms. The value of  $A_2^0 = -20.5 \text{ Ka}_0^{-2}$  for  $\text{HoFe}_{11}\text{Ti}$ , which can be contrasted to the value of  $A_2^0 = 300 \text{ Ka}_0^{-2}$  for  $R_2\text{Fe}_{14}\text{B}$  compounds.

From these results the following comments can be made. (i) Hydrogenation leads to a small increase ( $\sim 10\%$ ) of the  $4f$ - $3d$  exchange interaction. (ii) Hydrogen atoms has been found to have a significant effect on the second-order crystal field parameter  $A_2^0$  ( $A_2^0 = -118 \text{ Ka}_0^{-2}$  for  $\text{HoFe}_{11}\text{TiH}$ ). This fact is not surprising since both hydrogen and nitrogen atoms enter into the  $2b$  interstitial sites in  $\text{ThMn}_{12}$ -type structure. The contribution of neighboring nitrogen ions to second-order crystal-field parameter  $A_2^0$  are positive and large [ $A_2^0 = 85 \text{ Ka}_0^{-2}$  for  $\text{HoFe}_{11}\text{TiN}$  (see Ref. 18) these data have been obtained on polycrystalline samples], while more negative value of  $A_2^0$  is derived for the hydride than for the initial single crystals.

Interstitial hydrogen atoms occupy sites adjacent to the rare earth along the tetragonal  $c$  axis creating a strong change of crystal field at the position of  $R$  ions. On the other hand,  $R$  ions have asymmetric  $4f$  electronic shell, which orientation depend on symmetry and value of crystal field. Interaction between orbital moment of  $4f$  shell and crystal field modified by hydrogenation causes strong change of magnetic anisotropy, which was observed in our experiment.

We are very grateful to K.P. Skokov, V.V. Zubenko, I.V. Telegina, and W. Suski for the preparation and control of the single crystals, and V.N. Verbetsky and A.A. Salamova for hydrogenation of the sample. The work has been supported by the Federal Program on Support of Leading Scientific Schools 00-15-96695 and RFBR Grant No. 99-02-17821.

\*Corresponding author. Email address: nikitin@rem.phys.msu.su  
<sup>1</sup>M. Yamada, H. Kato, H. Yamamoto, and Y. Nakagawa, Phys. Rev. B **38**, 620 (1988).  
<sup>2</sup>J.F. Herbst, Rev. Mod. Phys. **63**, 819 (1991).  
<sup>3</sup>*Supermagnets: Hard Magnetic Materials*, edited by G.J. Long and F. Grandjean, Vol. 331 of *NATO Advanced Study Institute*,

Series C: Mathematical and Physical Sciences (Kluwer Academic, Dordrecht, 1991).

<sup>4</sup>B. Garcia-Landa, P.A. Algarabel, M.R. Ibarra, F.E. Kayzel, and J.J.M. Franse, Phys. Rev. B **55**, 8313 (1997).

<sup>5</sup>B.-P. Hu, H.-S. Li, J.M.D. Coey, and J.P. Gavigan, Phys. Rev. B **41**, 2221 (1990).

- <sup>6</sup>C. Abadia, P.A. Algarabel, B. Garcia-Landa, A. del Moral, N.V. Kudrevatykh, and P.E. Markin, *J. Phys.: Condens. Matter* **10**, 349 (1998).
- <sup>7</sup>D. Fruchart and S. Miraglia, *J. Appl. Phys.* **69**, 5578 (1991).
- <sup>8</sup>J.M.D. Coey, *Rare-earth Iron Permanent Magnets* (Clarendon Press, Oxford, 1996).
- <sup>9</sup>D. Bonnenberg, E. Burzo, H.R. Kirchmayr, T. Nakamichi, and H.P.J. Wijn, in *Landolt-Bornstein New Series, Vol. III/19i2* (Springer, Berlin, 1992), p. 314.
- <sup>10</sup>S.A. Nikitin, I.S. Tereshina, V.N. Verbetsky, and A.A. Salamova (unpublished).
- <sup>11</sup>I.S. Tereshina, S.A. Nikitin, T.I. Ivanova, and K.P. Skokov, *J. Alloys Compd.* **275-277**, 625 (1998).
- <sup>12</sup>A. Apostolov, R. Bezdushnyi, N. Stanev, R. Damianjva, D. Fruchart, J. Soubeyroux, and O. Isnard, *J. Alloys Compd.* **265**, 1 (1998).
- <sup>13</sup>Z. Arnold, J. Kamarad, O. Mikulina, B. Garcia-Landa, C. Abadia, M.R. Ibarra, and N.V. Kudrevatykh, *J. Magn. Magn. Mater.* **196-197**, 748 (1999).
- <sup>14</sup>E.B. Boltich, B.M. Ma, L.Y. Zhang, F. Pourarian, S.K. Malik, S.G. Sankar, and W.E. Wallace, *J. Magn. Magn. Mater.* **78**, 364 (1989).
- <sup>15</sup>X.C. Kou, T.S. Zhao, R. Grossinger, H.R. Kirchmayr, X. Li, and F.R. de Boer, *Phys. Rev. B* **47**, 3231 (1993).
- <sup>16</sup>J. Wang, G. Wu, N. Tang, D. Yang, F. Yang, F.R. de Boer, Y. Janssen, J.C.P. Klaasse, E. Brück, and K.H.J. Buschow, *Appl. Phys. Lett.* **76**, 1170 (2000).
- <sup>17</sup>M.D. Kuz'min, L.M. Carcia, M. Artigans, and J. Bartolome, *Phys. Rev. B* **54**, 4093 (1996).
- <sup>18</sup>Y.-c. Yang, X. Pei, H. Li, X. Zhang, L. Kong, Q. Pan, and M. Zhang, *J. Appl. Phys.* **70**, 6574 (1991).